Title

RIGOROUS AND SHORT-CUT DESIGN CALCULATIONS FOR GAS ABSORPTION INVOLVING LARGE HEAT EFFECTS PART II. RAPID SHORT-CUT DESIGN PROCEDURE FOR PACKED GAS ABSORBERS

Author

Stockar, Urs V.

Publication Date

1976-09-01

Submitted to Industrial and Engineering
Chemistry, Fundamentals

LBL-5274
Part II
Preprint

RIGOROUS AND SHORT-CUT DESIGN CALCULATIONS FOR GAS ABSORPTION INVOLVING LARGE HEAT EFFECTS PART II. RAPID SHORT-CUT DESIGN PROCEDURE FOR PACKED GAS ABSORBERS

Urs v. Stockar and Charles R. Wilke

September 1976

Prepared for the U. S. Energy Research and
Development Administration under Contract W-7405-ENG-48

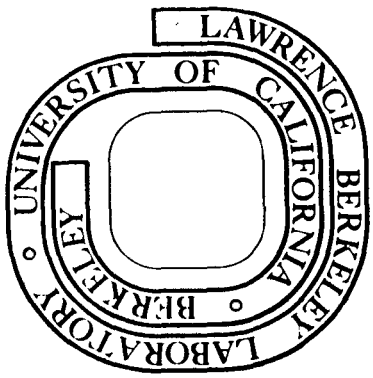

DISCLAIMER

RIGOROUS AND SHORT-CUT DESIGN CALCULATIONS FOR GAS ABSORPTION INVOLVING LARGE HEAT EFFECTS

PART II. RAPID SHORT-CUT DESIGN PROCEDURE FOR PACKED GAS ABSORBERS *

by

Urs v. Stockar

and

Charles R. Wilke
Lawrence Berkeley Laboratory
and
Department of Chemical Engineering
University of California
Berkeley, California 94720

This work was done with support from the U.S. Energy Research and and Development Administration. Any conclusions or opinions expressed in this report represent solely those of the author(s) and not necessarily those of the Lawrence Berkeley Laboratory nor of the U.S. Energy Research and Development Administration.

Abstract

A short-cut design procedure was developed allowing the quick approximate design of non-isothermal packed gas absorption columns by hand. The method is not based on simplifying assumptions but on a correlation of a large number of rigorously obtained liquid temperature profiles. The rigorous computations include a wide range of system properties and operating conditions. Correlation of the liquid temperature profiles was possible by correlating the temperature of the exit liquid and a temperature associated with the internal temperature maximum separately. Also, the need for graphical integration in cases with equilibrium lines curved due to the temperature variations was eliminated by replacing the curved equilibrium line by two straight lines and correlating the slopes of those lines. The proposed method is more reliable than the conventional approximate calculation methods based on simplifying assumptions and is often even less time consuming.

I. INTRODUCTION

In Part I of this study, a new calculational procedure was proposed for the rigorous treatment of packed gas absorption columns allowing for all heat effects, based on a dynamic solution employing rate equations derived from the film factor concept. It was demonstrated that heat effects render the conventionally recommended short-cut design procedures inadequate and unreliable even for preliminary design purposes, and the need for a more reliable quick design procedure accounting for the heat effects correctly was recognized.

Despite numerous efforts it was not possible to approximate the rigorous solutions by semitheoretical models simple enough to be solved manually. Therefore, an empirical approach was adopted to develop a short-cut method by correlating rigorously computed liquid temperature profiles by hypothetical systems covering a wide range of physical properties and operating conditions.

II. CORRELATION OF LIQUID TEMPERATURE PROFILES

Figure 1 shows typical liquid temperature profiles through the packing which are obtained by the rigorous computation for various operating conditions and system properties listed in Table 1. The profiles exhibit a large variety of shapes which may or may not have maxima and inflection points and may be curved upwards, downwards, or both. To confine those profiles to more regular patterns they were split into two superimposed portions (Fig. 6). One portion is linear and is obtained by first plotting the profile against the liquid concentration and then drawing a straight line

Table 1

Specifications for sample temperature profile calculations, Fig. 1

Profile	Solute	H_{OS} cal/mole	P_A^o (20°C, X=o) mmHg/mole fraction	Recovery fraction	$Y^*_{B,1}$	L/G	$H_{G,A}$ ft.	H_L (25°C) ft.	$H_{G,B}$ ft.	$H_{G,Q}$ ft.
a	Acetone[1]	7653	1285.6	0.90	Saturated	2.47	1.37	0.99	0.9	1.08
b	Ammonia[2]	8220	612.8	0.99	0	1.88	2.0	1.25	2.0	2.32
c	"A"[3]	8220	131.4	0.99	0	1.88	2.0	1.25	2.0	2.32
d	"A"	2000	612.8	0.99	0	1.88	2.0	1.25	2.0	2.32
e	"A"	8220	612.8	0.99	0	1.75	1.5	0.94	1.5	1.74

Common Specifications: Solvent is water, $Y_{A,1} = 0.06$, $T_{L,2} = T_{G,1} = 15°C$, $X_{A,2} = 0$

Explanations: 1 = The properties of acetone used in this calculation are the ones given in the appendix, which also states the other exact specifications for this run. A rigorously computed Y-X diagram for this case may be found in Part I of this study.

2 = The solubility data for ammonia has been idealized using a constant activity coefficient derived from a liquid concentration of 4 mole-% and an activation energy of 8.23 kcal.

3 = Substance "A" is a hypothetical solute with some variable properties as shown in the table, but otherwise identical to ammonia as described above.

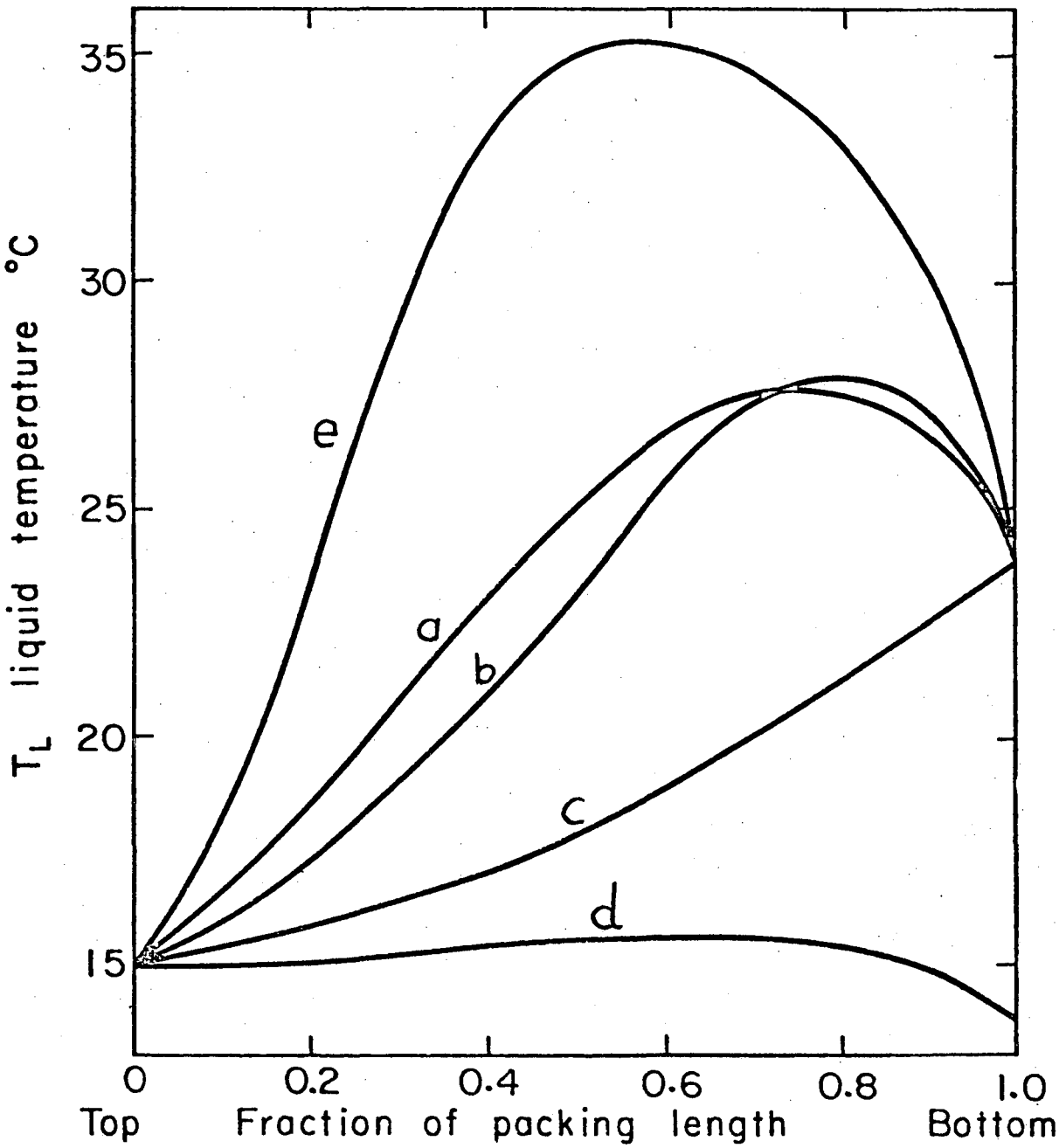

XBL753-2517

Fig. 1. Liquid temperature profiles for different operating conditions and system properties.

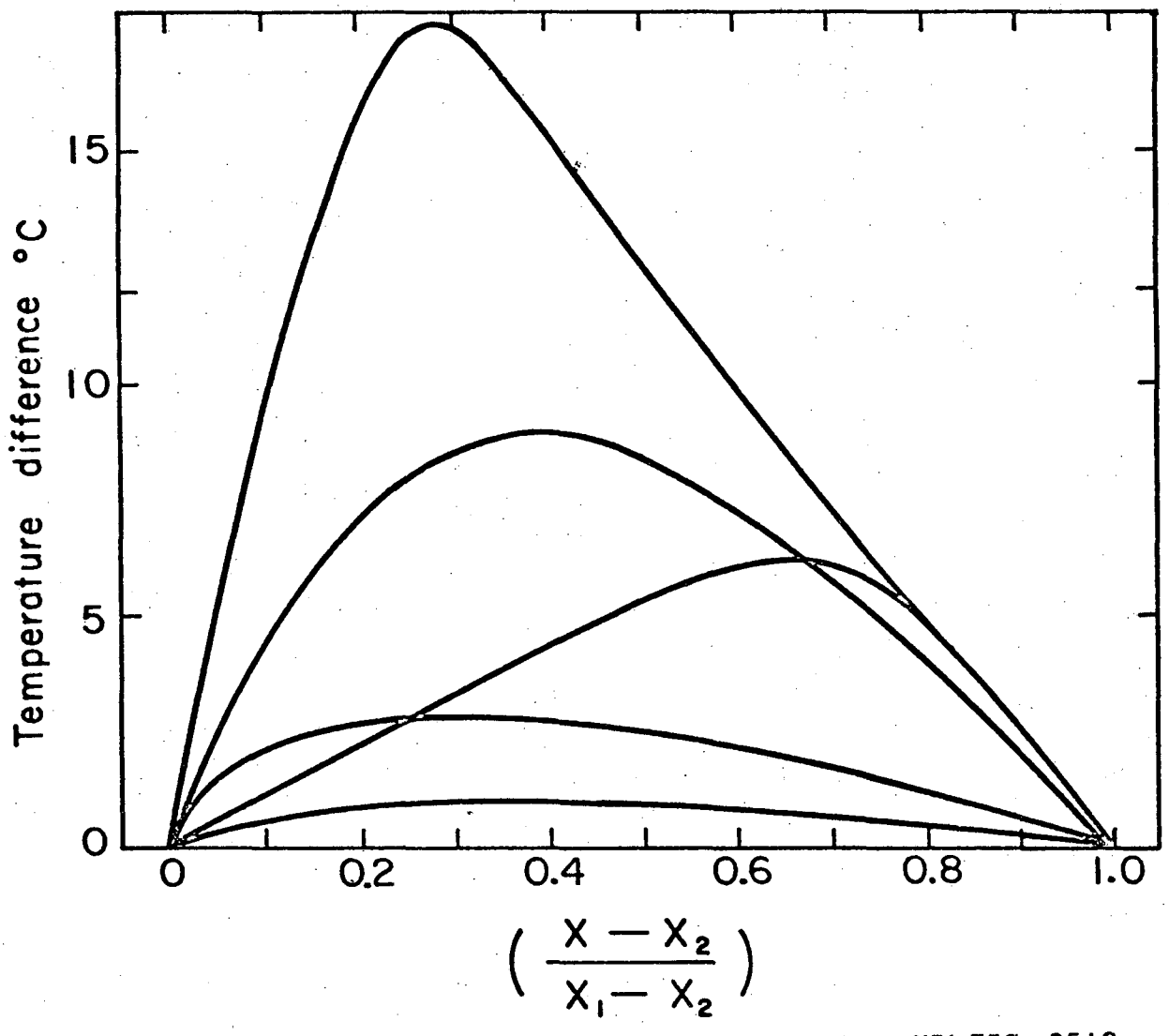

Fig. 2. Convex portions of liquid temperature profiles at different operating conditions.

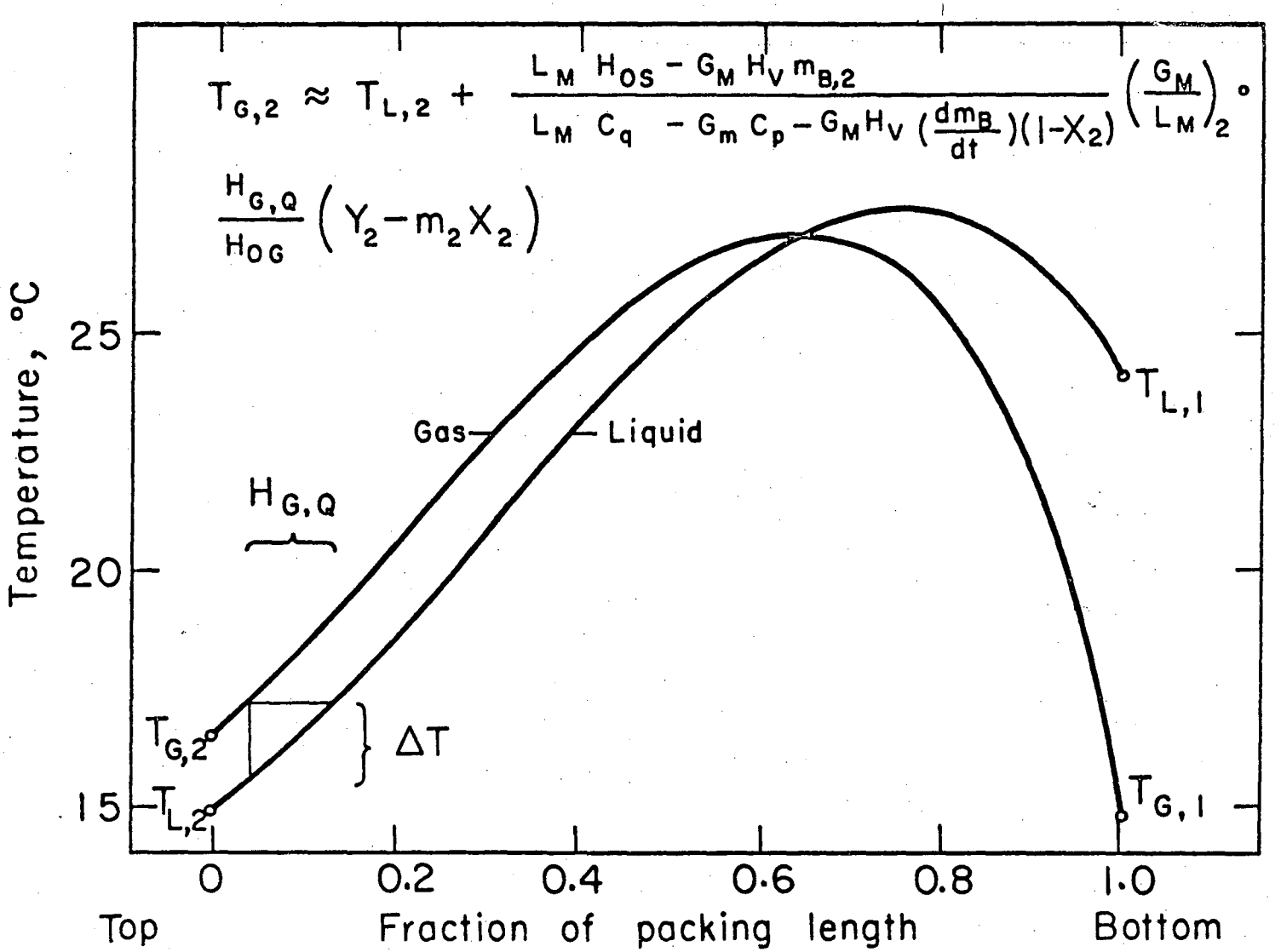

Fig. 3. Semitheoretical model for prediction of $T_{G,2}$. XBL753-2508

from the beginning to the end point of the profile. The remaining portion is a convex curve which does not appear to change its shape too drastically. Figure 2 depicts the convex portions of the profiles shown in Fig. 1 plotted against a normalized liquid concentration. The linear portion and the superimposed convex portion were correlated separately. The liquid temperature profiles could thus be characterized by two main elements: the temperature of the exit liquid, which is associated with the linear portion of the profile, and the internal temperature maximum, being associated with the convex portion.

1. Linear Part of Liquid Temperature Profile

Since the linear portion of the liquid temperature profile simply consists of a straight line connecting the liquid inlet and outlet temperatures, its prediction calls only for the correlation of the latter. This may be accomplished by an enthalpy balance around the column based on a reasonable guess of the gas outlet temperature and on the assumption that the exit gas is saturated with solvent. Although this sounds easy, it is important to recognize that a small error in the estimation of the product gas temperature might cause a large error in the liquid outlet temperature, because it could involve a substantial error in the estimation of solvent evaporation. The

estimation of the outlet gas temperature must therefore be grounded on a rational basis and should not simply be set arbitrarily a few degrees higher than the liquid feed temperature.

The fact that the gas and liquid temperature profiles are found to be almost parallel and straight at the top end of the tower (Fig. 3) might serve as such a basis. It follows that towards the upper end, the two profiles on Fig. 3 are separated horizontally by one height of a heat transfer unit. Thus the temperature difference between the profiles, i.e. their vertical separation on Fig. 3 can be computed from the height of a heat transfer unit, provided that the initial slope of the profiles is known. This may be estimated through a differential enthalpy balance at the end of the tower under the assumption, that not only the driving force for heat transfer, but also the one for solvent transfer approaches a constant value towards the dilute end of the packing. From:

$$dT_L \approx \frac{H_{OS}}{c_q} dX_A + \frac{G_M}{L_M c_q} H_V dY_B + \frac{G_M}{L_M c_q} c_p dT_G$$

it follows with

$$dY_B \approx dY_B^* \approx dm_B (1-X_A) - m_B dX_A$$

and

$$dT_G \approx dT_L \ :$$

$$\left(\frac{dT_L}{dX_A}\right)_2 \approx \frac{L_M H_{OS} - G_M H_V m_{B2}}{L_M c_q - G_M c_p - G_M H_V (1-X_{A,2}) (dm_B/dT_L)_2} \qquad (1)$$

But since

$$\frac{dX}{dz} \approx \frac{Y - Y^*}{H_{OG}} \left(\frac{G_M}{L_M}\right) \ ; \qquad (2)$$

Equation 1 can be used to predict the gas product temperature as follows:

$$T_{G2} \approx T_{L2} + \left(\frac{dT_L}{dX_A}\right)_2 \left(\frac{G_M}{L_M}\right)_2 \frac{H_{OG,Q}}{H_{OG,A}} \left(Y_{A2} - m_A X_{A2}\right) \qquad (3)$$

where

m_{B2} = slope of the equilibrium line for solvent at T_{L2}

$\left(\frac{dm_B}{dT_L}\right)_2$ = temperature coefficient of slope for solvent at T_{L2}

Equations 1 and 3 were used to predict gas product temperatures and through a heat balance corresponding liquid product temperatures for about 90 rigorously computed hypothetical design cases. The rigorous liquid outlet temperature could be predicted within a standard deviation of 1.2°C and a statistical test showed that there was no significant difference between the predicted and the rigorously computed liquid product temperatures. It may be concluded that it is generally possible to predict the linear portion of the temperature profile.

2. Convex Part of Liquid Temperature Profile

The most important characterization of the convex curves (compare Fig. 2) consists of the magnitude of their maxima, which vary in an extremely complicated fashion with the independent variables over a wide range.

To correlate the curves, the dependency of these maxima on the independent variables was investigated by rigorously computing a carefully selected set of over 90 hypothetical design cases. The range covered by these calculations is given in Table 2 and includes wide variations in most of the revelant system properties and operating conditions. Main considerations used to define sensible limits to this range include the following:

a) The $\frac{mG}{L}$ - factor has been varied from the maximum values given by pinchpoints between the equilibrium and operating lines down to values where the heat effects were subdued by the heat capacity of the high solvent flow rate. In many cases, the temperature profile becomes dominated by the heat of solution alone as $\frac{mG}{L}$ gets very low because an increase in the L/G ratio enhances gas absorption strongly but not solvent evaporation (2). Solvent evaporation may then be safely neglected as a heat effect and the temperature profile can be estimated accurately and easily using the simple adiabatic model discussed in Part I. This condition defined the lower limit of $(\frac{mG}{L})$ in such cases, of which Run c, Table 1, is an example.

Table 2

Range Covered by the Hypothetical Design Computations

INDEPENDENT VARIABLE	RANGE
Operating Conditions	
$(L/G)_2$ ratio	1.23 - 4.18
$Y_{A,1}$	0.06 - 0.15
$Y_{B,1}$	0 - saturated
$T_{L,2}$	10° - 50°C
$T_{G,1}$	10° - 50°C
Recovery fraction	0.9 - 0.99
System Properties	
Henry's constant at feed temperature	0 - 1000 mm Hg/mole fraction
Henry's constant within the column	0 - 1400 mm Hg/mole fraction
Heat of solution (integral)	0 - 14,000 cal/mole
Heat of evaporation	10,000 - 11,000 cal/mole
Roult's constant for solvent at feed temperature	0 - 100 mm Hg/mole fraction
Packing Properties	
$H_{G,A}$	0.8 - 4.0 ft
$H_{G,B}$	0.6 - 5.0 ft
$H_{G,A}/H_L$	1.0 - 4.0
$h_G a$	38 - 230 cal/(hr)(sq.ft)
$h_L a$	160 - 25,000 cal/(hr)(sq.ft)
H_L	1.0 - 4.0 ft

Explanation of Subscripts

A	Solute
B	Solvent
G	Gas
L	Liquid
1	Foot of column
2	Top of column

b) The apparent Henry's Law constants were varied from zero to 1400 mmHg. This corresponds to a maximum K value of 1.75 and includes gases with high enough solubilities to allow a reasonably easy absorption at atmospheric pressure. Examples include the absorption of polar solvents in water such as ammonia, acetone, propanol, ethanol and other lower alcohols. Systems outside this range, such as ammonia at elevated temperatures, would require such a high L/G ratio for a reasonable degree of absorption that the conditions discussed in paragraph (a) would apply.

c) Heats of solutions were taken into account up to 14 kcal/mole. This includes even highly exothermic physical absorption such as that for aqueous solutions of methanol, formaldehyde, ammonia, sulfur dioxide, etc.

d) The gas phase heights of mass and heat transfer units were varied to allow for Schmidt Numbers in the gas phase ranging from 0.6 to 3 and Prandtl Numbers from 0.5 to 1.2. In the liquid phase Schmidt Numbers were assumed to vary from 200 to 4000 and the ratios of Prandtl and Schmidt Numbers from 0.005 to 0.05, which includes such mixtures as ammonia in water, CO_2 in water, polar organic solvents in water, lower alcohols in ethanol and benzene in heptane.

The main arbitrary limitations of the range covered by the calculations are: (1) atmospheric pressure was assumed in all calculations although no significant effect of pressure would be expected below 10 atm., (2) the investigation is limited to gas concentrations below 15 mole-%, (3) the recovery fractions were limited to the important range between 90 and 99%, and (4) water was considered to be the most important solvent, and the correlation will yield the most accurate results with aqueous solutions, although the effect of solvent properties has been incorporated to a certain extent.

The maximum values of the convex portions of the temperature profiles were evaluated for the 90 hypothetical design cases on the basis of the rigorous computer profiles and then correlated as shown in Fig. 4. In this graph, the function of the maximum value ΔT_{max} which is given in the upper left part of the figure was plotted against the expression on the abscissa. The points shown are for 99% recovery. The lines represent the best fit for three recovery fractions of a mathematical expression, Eq. 4, which has been fitted to the rigorously computed data points using a multidimensional nonlinear regression technique:

$$\Delta T_{max} = 10.039 \left\{ \exp(2.17.10^{-3}\ \xi \cdot \Delta Y \cdot R_f - 1.57.10^{-3}\ \xi .\ \Delta Y) - 1 \right\} \cdot m_A^{0.995}\ m_B^{0.443}\ \exp\left(0.36\ \frac{Y_{B1}}{Y_B^*} \right) \left(\frac{H_{OG,A}}{H_{OG,B}} - 0.39 \right)\ 0.66 \left(\frac{H_{OG,A}}{H_{OG,Q}} \right)^{0.4} \tag{4}$$

$$\xi = \frac{H_{OS} H_V}{c_q^2} \left(\frac{G_M}{L_M} \right)^2 \cdot \Delta Y \tag{5}$$

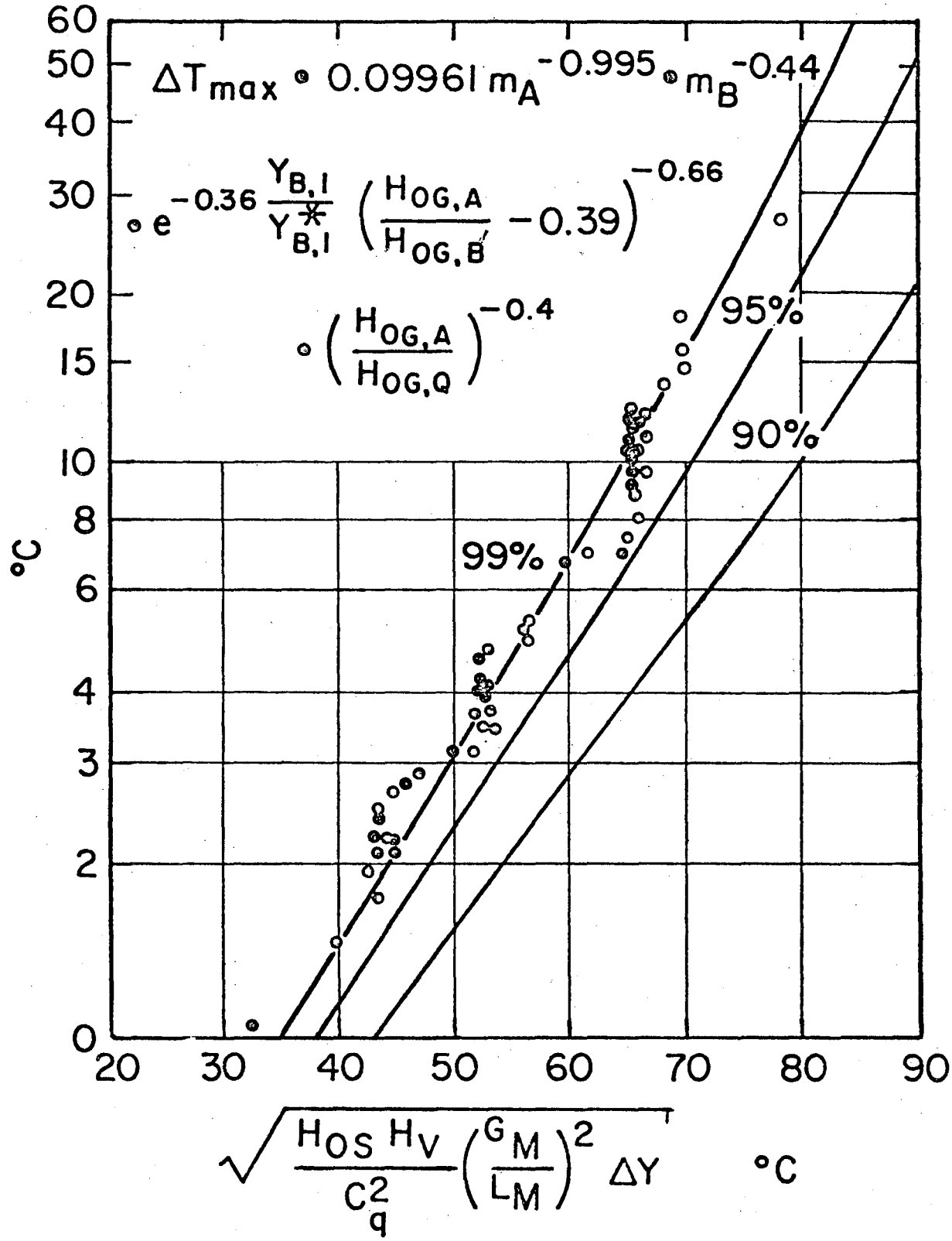

XBL 764-2793

Fig. 4. Correlation of ΔT_{max}.

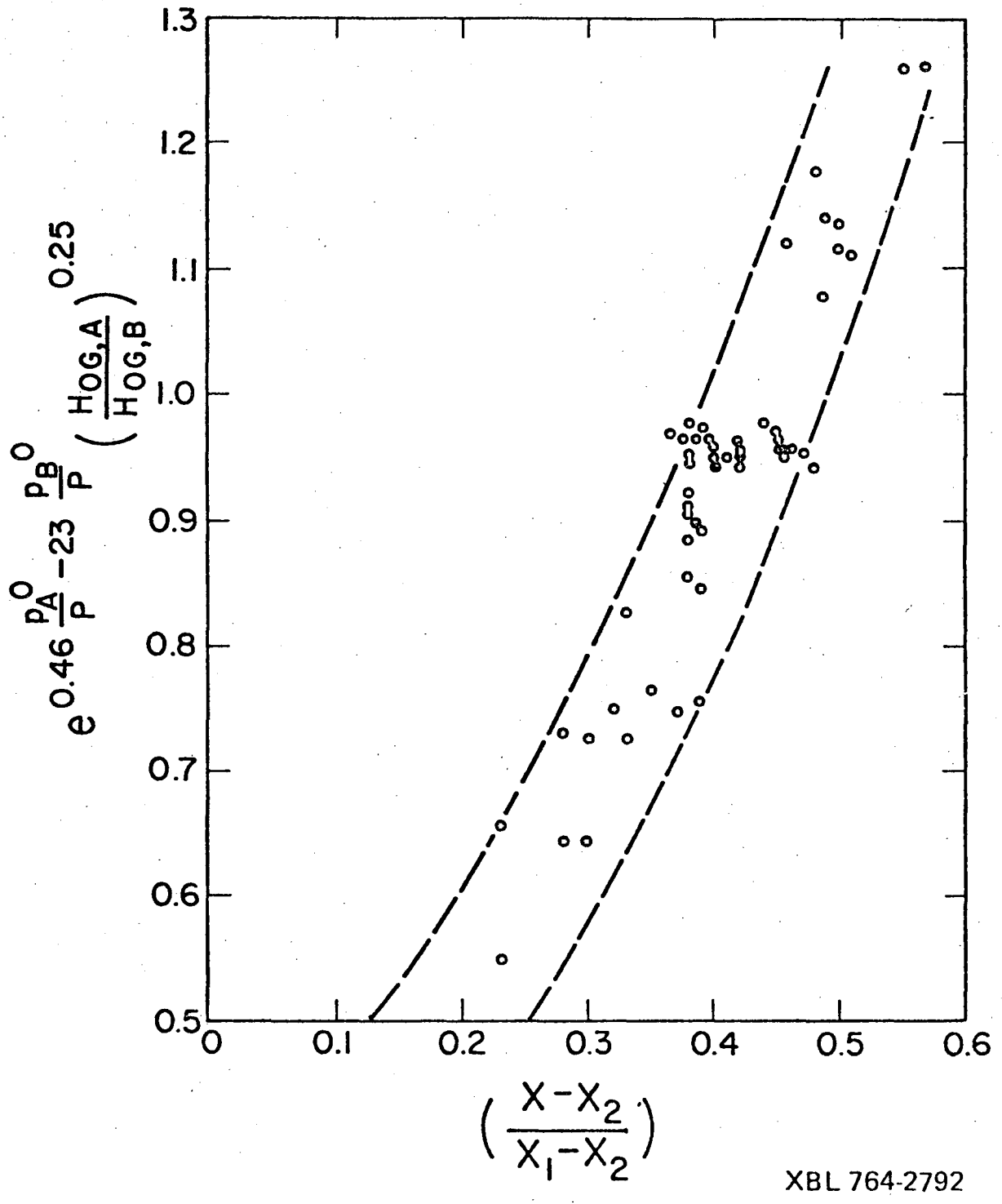

Fig 5. Correlation of liquid concentration at which ΔT_{max} occurs.

The function ξ, the root of which appears on the abscissa of Fig. 4 represents the product of a so called heating and a so called cooling potential. These potentials are a measure of the possible temperature rise in the liquid phase due to the heat of solution and the possible amount of cooling due to solvent evaporation. Since the generation of a temperature bulge may be attributed to the interaction of such heating and cooling effects, it can be anticipated that the product of correspondingly defined potentials will play a major role in the determination of the magnitude of the temperature bulge. The correlation, as represented by Fig. 4 or Eq. 4, correlates the rigorously computed values of the maximum temperature of the convex curves within a standard deviation of 0.7°C for our 90 design cases.

By means of a further multidimensional regression analysis it was also possible to obtain a correlation for the normalized liquid concentration at which the temperature maximum of the convex portion occurs (Fig. 5). The location of the maximum does not vary too drastically and the end results of the approximate design calculations were found to be much less sensitive to the location of the maximum than to its magnitude. It was therefore decided for the sake of simplicity to approximate the convex temperature profiles by a synthetic mathematical curve with the maximum fixed at a normalized concentration of 0.4.

3. Application of the Correlations

The liquid temperature as a function of the concentration may now be approximated by an empirically constructed, synthetic temperature profile as shown in Fig. 6. Its mathematical representation is as follows:

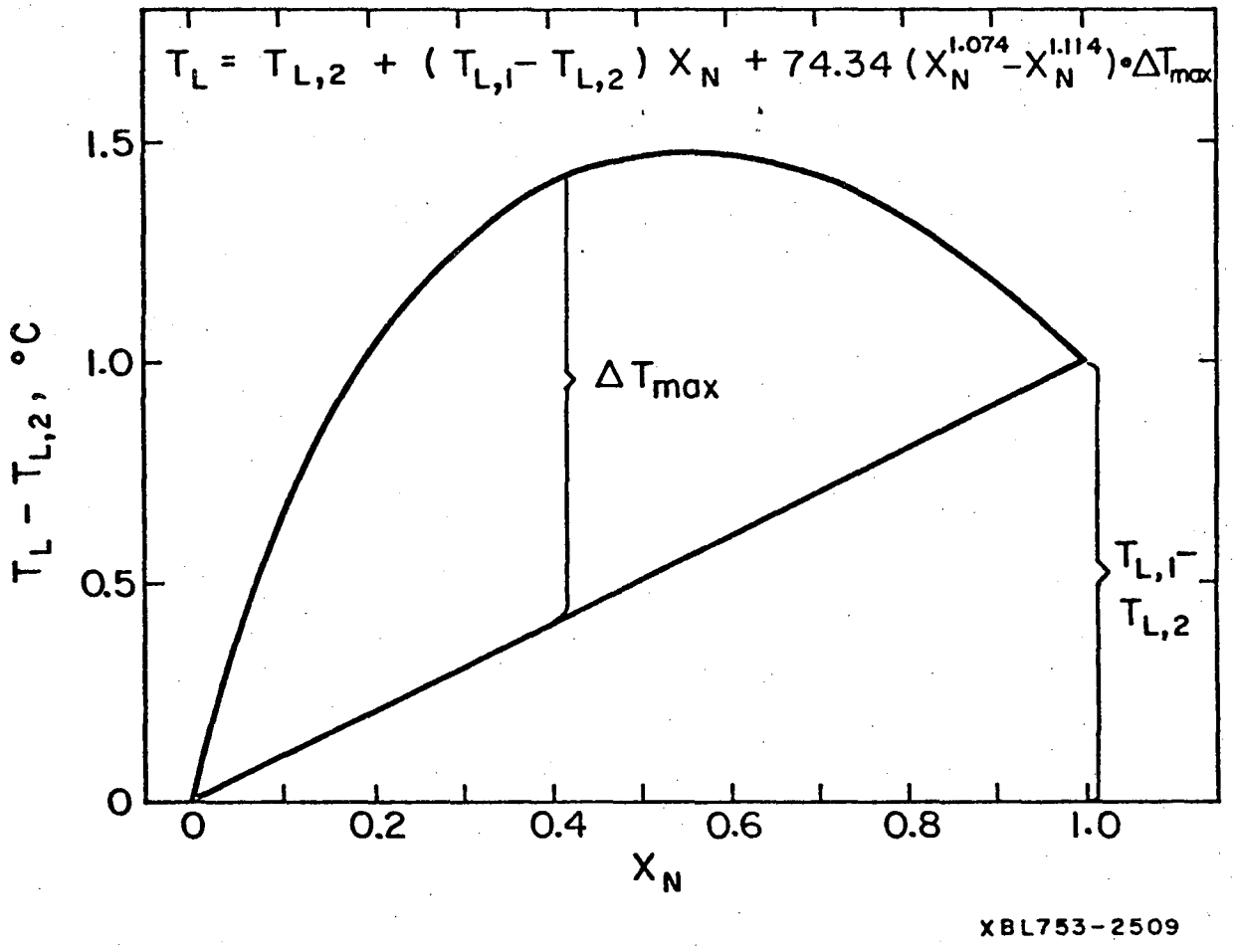

Fig. 6. Empirically constructed (synthetic) liquid temperature profile.

$$T_L = T_{L,2} + (T_{L,1}-T_{L,2})\ X_N + 74.34\ (X_N^{1.074}-X_N^{1.114})\ \cdot\ \Delta T_{max} \qquad (6)$$

The first two terms on the right side of the equation constitute the linear portion. The only unknown, the temperature of the product solution, $T_{L,1}$, is to be estimated via the temperature of the exit gas by means of Eqs. 1 and 3. The last term of Eq. 6 represents the mathematical model of the convex portion, the only unknown parameter is the value of its maximum, ΔT_{max}, which may be estimated employing the correlation just discussed. The exponents of the last term are fixed so that the maximum of the convex curve occurs at $X_N = 0.4$. If an especially accurate estimation of the liquid temperature profile is warranted, one may want to adjust the two exponents and thereby shift the maximum to the normalized concentration predicted by Fig. 5.

If it is applied at a few values of the liquid concentration, Eq. 6 yields corresponding temperature values which may serve to evaluate the equilibrium gas concentration, Y^*, as a function of the liquid concentration. This procedure will yield a good approximation of the rigorous equilibrium line accounting for all heat effects. The required number of transfer units and the tower height may then be computed on the basis of a conventional X-Y diagram by graphical integration.

III. ANALYTICAL INTEGRATION

1. Effective Average Slope of Equilibrium Line

In the new design technique outlined thus far, allowing the quick approximate design of adiabatic absorption towers, the

graphical integration is by far the most time consuming step. Therefore, a way was devised to by-pass it by means of an analytical procedure without much loss of accuracy. Provided that 1) the operating line is straight, 2) that there is only negligible net molar flux through the films, and 3) that also the equilibrium line is straight, the integration can be performed analytically as first shown by Colburn (1):

$$N_{OG} = \frac{\ln\left\{\left(1 - \frac{mG_M}{L_M}\right)\left(\frac{Y_1 - mX_2}{Y_2 - mX_2}\right) + \left(\frac{mG_M}{L_M}\right)\right\}}{1 - \frac{mG_M}{L_M}} \qquad (7)$$

The first two conditions, which are of course not independent from each other, are fulfilled within the low concentration range of our investigation at least to a certain extent. The third, however, is strongly violated by the weird shapes of nonisothermal equilibrim lines.

As the basis for a simplified calculation procedure the equilibrium line is broken down into two parts at its inflection point as shown in Fig. 7. In each part, the equilibrium curve is replaced by a straight line with a slope $\bar{m}$, which upon substitution into Eq. 7 yields the same number of transfer units as the graphical integration based on the curved equilibrium line. These effective average slopes $\bar{m}$ were calculated for an expanded set of well over 100 hypothetical design cases by performing the integration numerically and solving Colburn's equation numerically for m. The effective average slopes could be correlated to the initial slopes and the

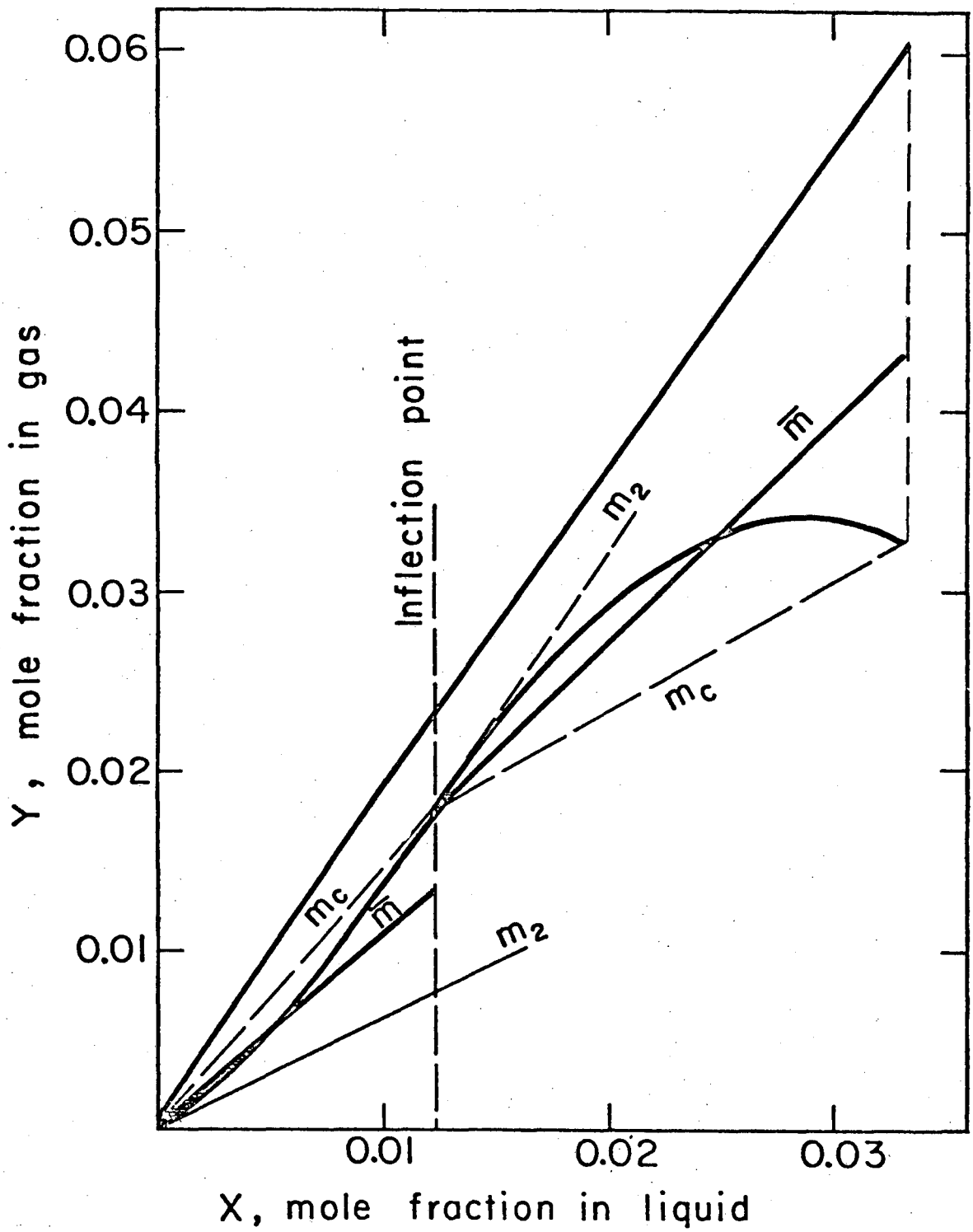

XBL753-2510

Fig. 7. Definition of effective average slopes of equilibrium line.

cord of the equilibrium line of the respective section (Fig. 7). Again based on nonlinear multidimensional regression techniques two such correlations were developed. One applies for the dilute section of the X-Y diagram, where the equilibrium line is curved concave upward.

$$\left[\frac{\bar{m}}{m_2} - 1\right]\left[\frac{Y_{ip} - Y_2^*}{Y_2 - Y_2^*}\right]^{0.1797} = 0.57776\left[\frac{m_c}{m_2} - 1\right]^{0.9229} \cdot \exp\left\{0.78022\left[\frac{Y_{ip}^* - Y_2^*}{Y_{ip} - Y_2^*}\right]\right\} \tag{8}$$

The other one is for the concentrated part with concave downward equilibrium lines:

$$\left[1 - \frac{\bar{m}}{m_{ip}}\right]\left[\frac{Y_1 - Y_{ip}^*}{Y_{ip} - Y_{ip}^*}\right]^{0.2281} = 0.48787\left[1 - \frac{m_c}{m_{ip}}\right]^{0.9298} \cdot \exp\left\{0.41362\left[\frac{Y_1^* - Y_{ip}^*}{Y_1 - Y_{ip}^*}\right]\right\} \tag{9}$$

Curves representing the above equations are given in Figs. 8 and 9, which also indicate the range of validity of these correlations. Figs. 8 and 9 allow a very rapid determination of the required depth of packing. If the effective average slope $\bar{m}$, after having been read from these charts, is substituted into the expression of Colburn, Eq. 7, a nearly correct number of overall transfer is obtained despite the curvature of the equilibrium line.

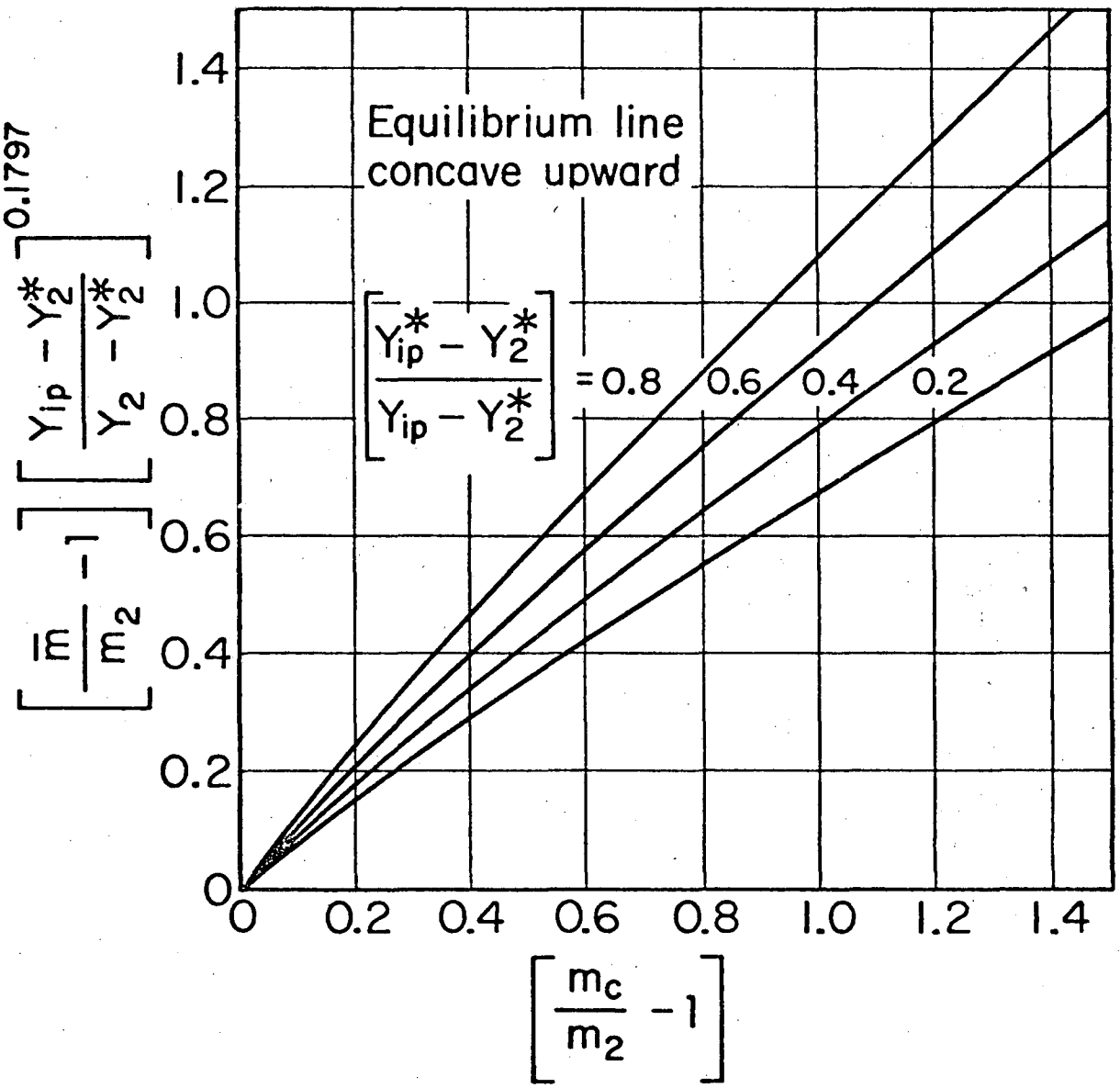

Fig. 8. Correlation of effective average slope $\bar{m}$ of equilibrium line. Dilute part of absorber.

XBL 763-2555

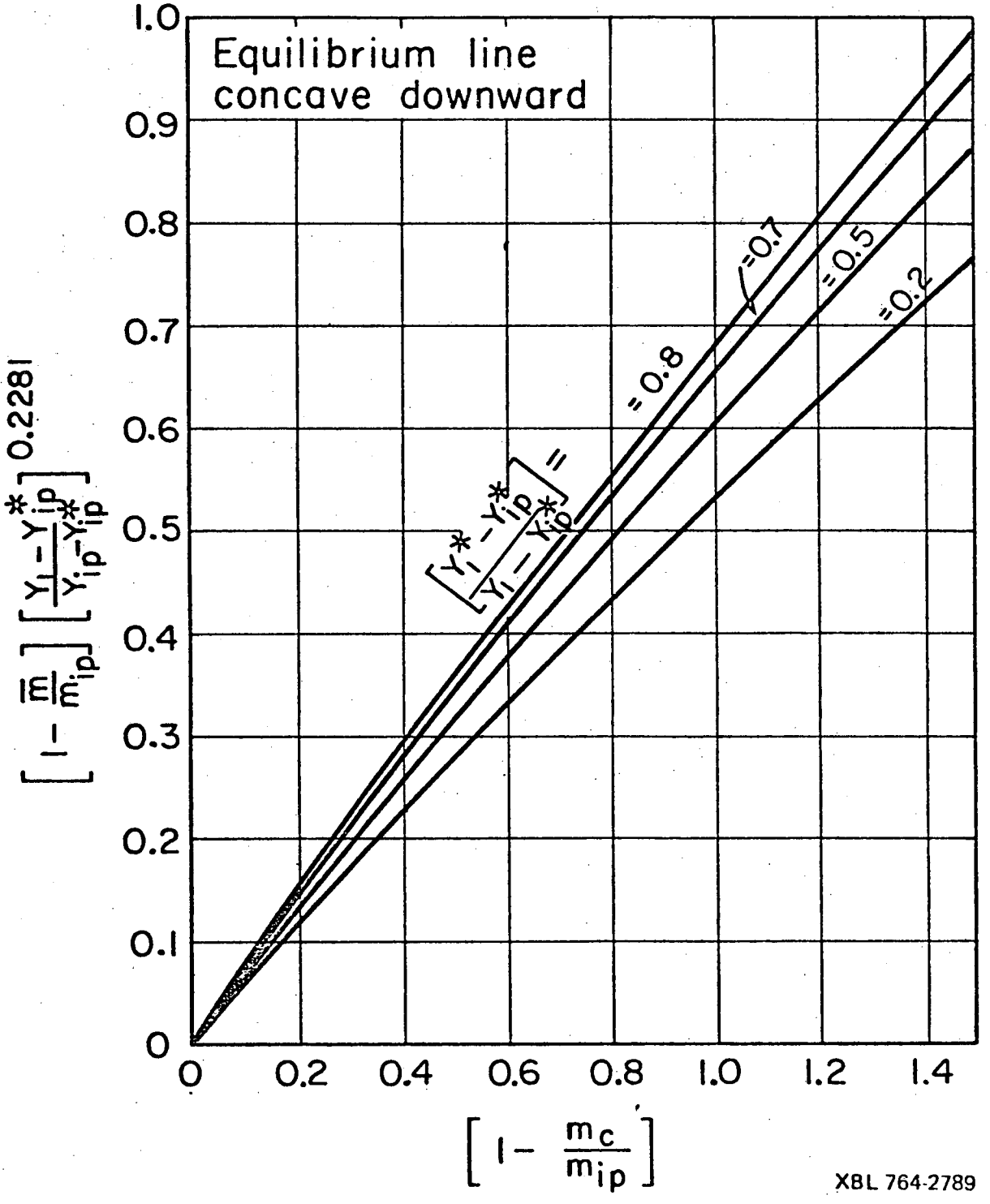

Fig. 9. Correlation of effective average slope $\bar{m}$ of equilibrium line. Concentrated part of absorber.

The overall height of a transfer unit may be computed from the individual gas and liquid heights of a transfer unit as usual:

$$H_{OG} = H_G + \left(\frac{mG_M}{L_M}\right) H_L \qquad (10)$$

It was found that the effective average value $\bar{m}$ read from Figs. 8 and 9 may also be used in Eq. 10 to compute H_{OG} without significant error.

2. Locating the Inflection Point

To use Figs. 8 and 9, the inflection point must be located on the design diagram to obtain the correct break-down of the equilibrium curve. Even if one assumes ideal solutions and a temperature profile given by Eq. 6, it is impossible to calculate the inflection point analytically. But it is possible to show that in this case the normalized concentration, at which the highest temperature occurs, only depends on $(T_{L,1} - T_{L,2})/\Delta T_{max}$. The same parameter was therefore used to correlate the inflection points. This correlation is given in Fig.10 and serves to locate the inflection point without trial and error. Alternatively, the following equation may be used to find the inflection point:

$$\left[\frac{X_{ip} - X_2}{X_1 - X_2}\right] = 0.3546 \exp\left(0.2438 \frac{T_{L,1} - T_{L,2}}{\Delta T_{max}}\right) - 0.0962 \qquad (11)$$

If $(T_{L,1} - T_{L,2})/\Delta T_{max}$ becomes large enough, the equilibrium line does not show an inflection point and the curve as a whole may then be replaced by a single straight line with a slope $\bar{m}$ given by Fig. 8. This is especially the case when the solvent is not volatile. Such examples may be calculated by the conventional

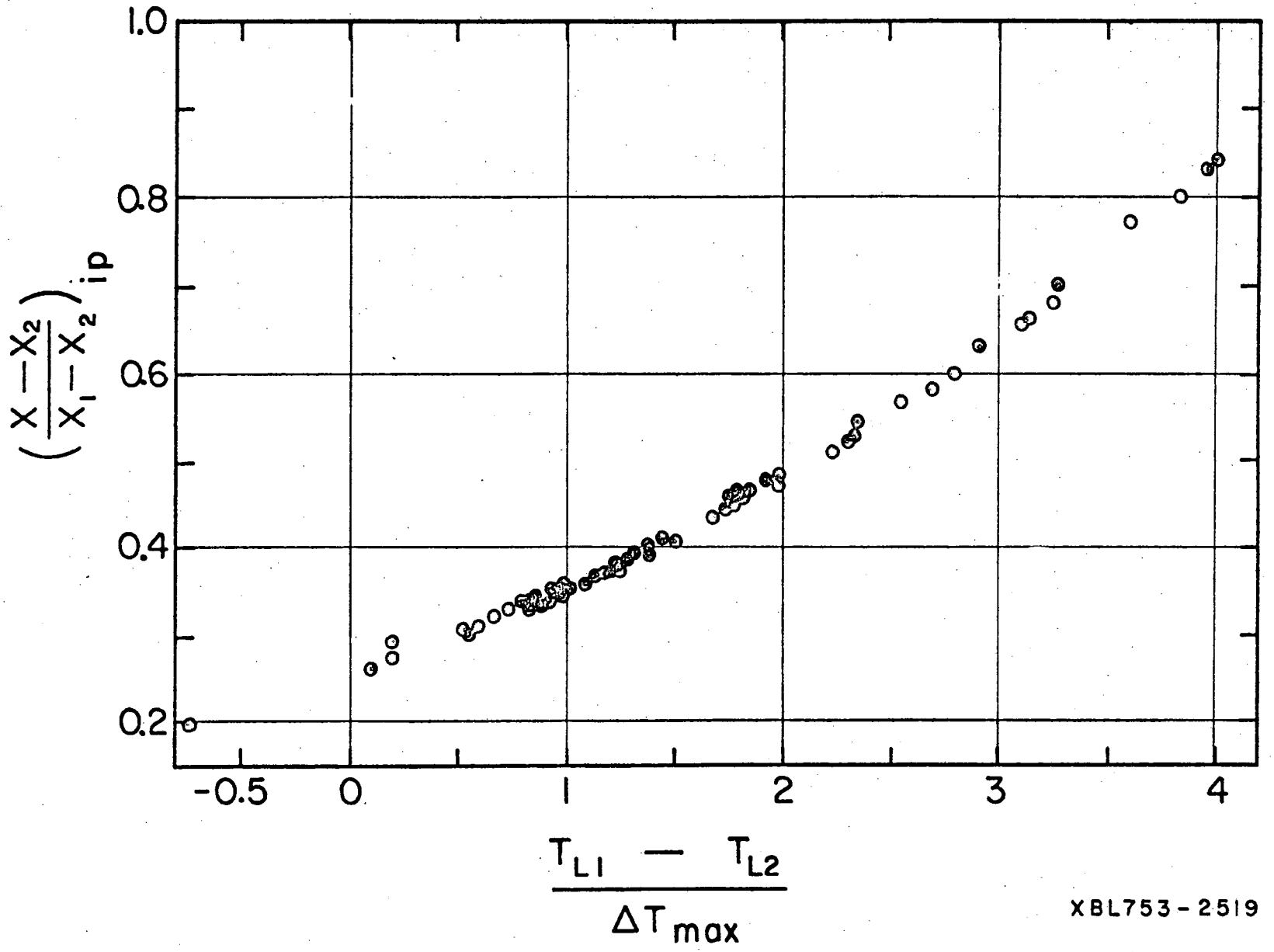

Fig. 10. Correlation of inflection point.

so called simple model of adiabatic gas absorption mentioned in Part I, but the integration can be performed much faster analytically on the basis of Fig. 8.

3. Corrections for Net Molar Flux through the Interface

If the net molar flux through the films are not nearly zero, the operating line will not only slightly be curved but its slope will also deviate from the L/G ratio, which violates an underlying assumption of Eq. 7. In computing the stripping factor $(\frac{mG_M}{L_M})$ it is advisable in such cases to substitute an average of the actual slope of the line which may be calculated conveniently from L_M/G_M on the basis of the film factor concept:

$$\left(\frac{L_M}{G_M}\right)_{eff} = \frac{dY}{dX} = \frac{L_M}{G_M}\,\frac{1 - tY}{1 - tX} \qquad (12)$$

Suitable average values have to be used for the flow rates, the concentrations and for t. Methods for estimating average values of t are reviewed in "Mass Transfer" (6).

Non-zero net molar flux invalidates yet another underlying assumption. The correct expression for the number of transfer units may be written in terms of the film factor concept in the following familiar form:

$$N_{OG} = \int_{Y_1}^{Y_2} \frac{Y_f^*}{1 - tY} \cdot \frac{dY}{Y - Y^*} \qquad (13)$$

Y_f^* is a film factor based on the overall driving force just as Y_{BM}^*, of which the former represents a generalization. In the derivation of Eq. 7, the term $Y_f^*/(1-tY)$ has been neglected since

it equals unity for equimolar counterdiffusion. This introduces an error for all other situations. If very accurate work is warranted, one may correct for this usually small error by breaking the integral of Eq. 13 down as follows (6):

$$N_{OG} = \int_{Y_1}^{Y_2} \frac{dY}{Y - Y^*} + \frac{1}{2} \ln \frac{1 - tY_1}{1 - tY_2} \qquad (14)$$

The integral on the right hand side of Eq. 14 has the analytical solution given by Eq. 7. The last term is the desired correction and was derived under the assumptions of constant average t through the tower and that the logarithmic mean in Y_f^* may be replaced by the arithmetic mean. The equation is analogous to the relation derived by Wiegand (3) for the special case of unidirectional diffusion of one component. Alternatively, the error may also be accounted for by employing a correlation developed in "Mass Transfer" (6).

IV. RESULTS

The accuracy of this new technique was compared with the conventional isothermal and simple adiabatic models by recalculating the 90 hypothetical design examples on the basis of the three approximations. It was already demonstrated in Part I of this study (Figs. 6 and 7) that a plot of the rigorous results for the tower height vs. the approximate estimations show excessive scattering as well as systematic deviations from the rigorous results for both the isothermal treatment and the

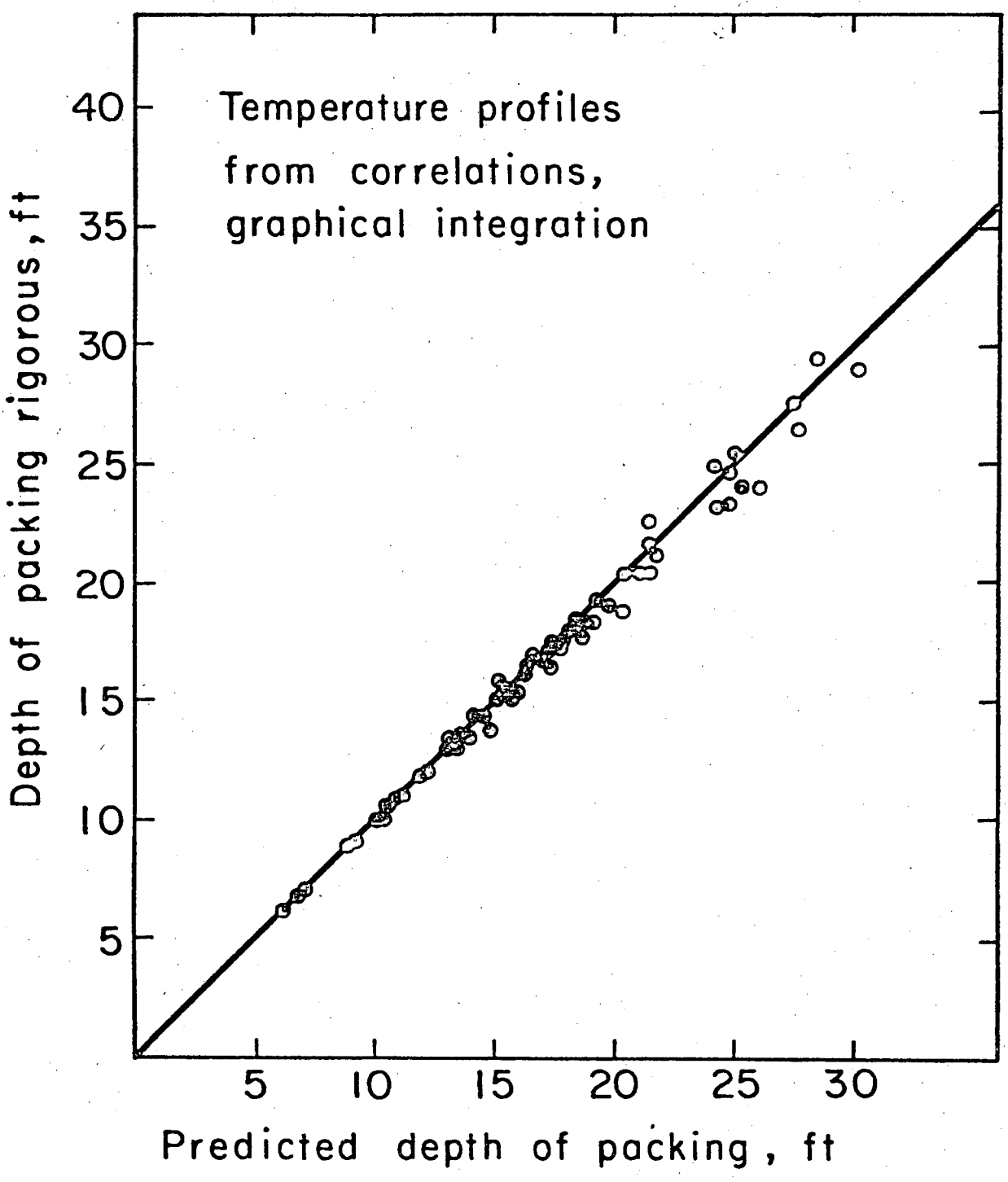

XBL753-2515

Fig. 11. Comparison between rigorous solution and suggested quick short-cut design procedure.

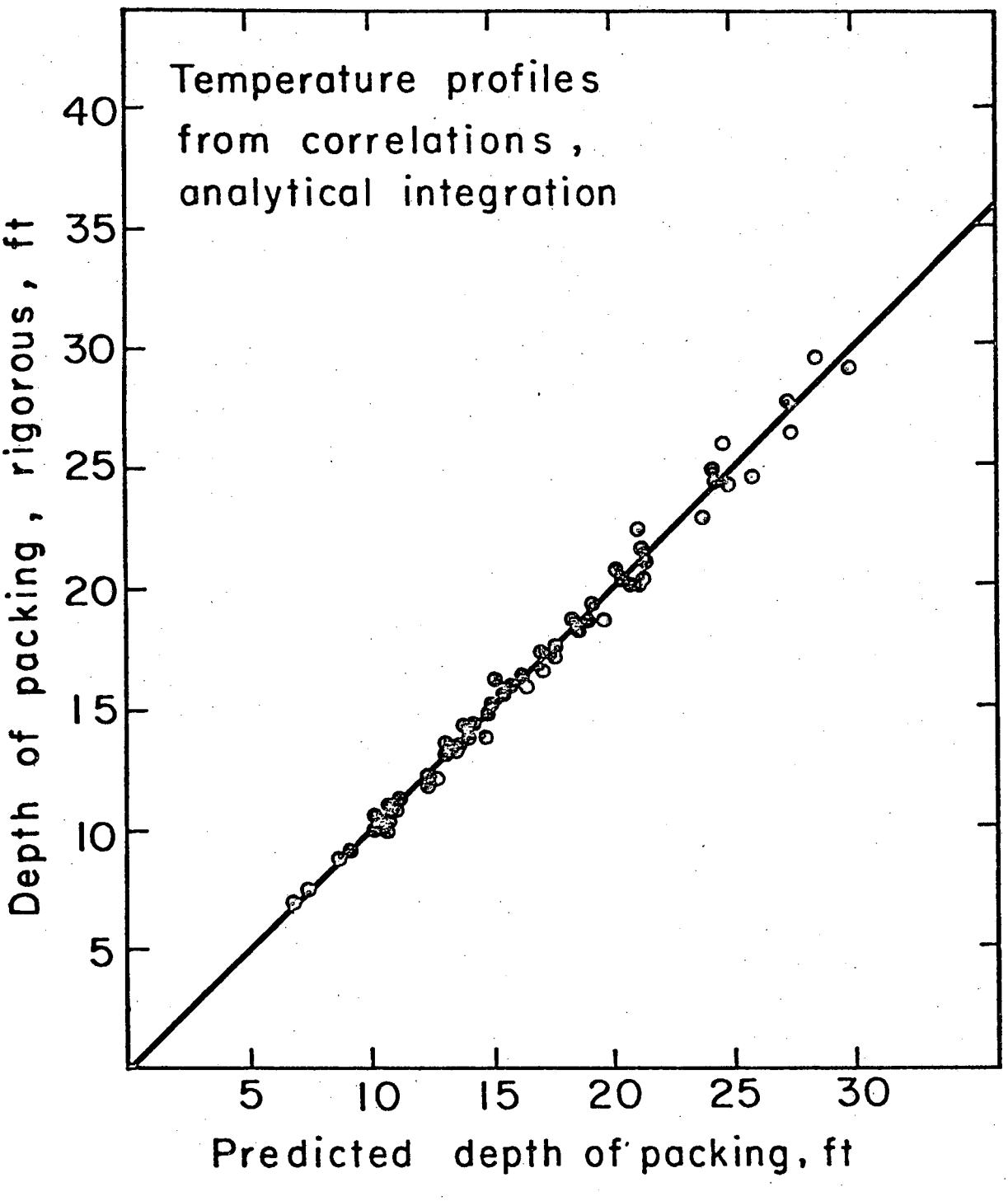

Fig. 12. Comparison between rigorous solution and suggested quick short-cut design procedure, analytical integration.

simple adiabatic model, thus indicating their unreliability. If we now apply the new method, all of the design cases may be estimated with a much better accuracy, as shown in Figs. 11 and 12, and scattering around the 45° line is reduced to an insignificant degree. The integration for N_{OG} was performed graphically for the results shown in Fig. 11, whereas the effective average equilibrium line slopes were employed in Eqs. 7 and 10 to obtain N_{OG} and H_{OG} for the results shown in Fig. 12. The fact that the results in Figs. 11 and 12 are almost the same illustrates the reliability of the analytical approach, which simply approximates the curved equilibrium line by two straight lines.

The standard deviation of the final comparison, Fig. 12, is 3%, and a statistical test has shown that no significant difference existed between the predicted values and the rigorously calculated results.

As an illustration, the proposed method was applied to a design problem selected from the textbook, "Mass Transfer" by Sherwood, Pigford, and Wilke (4). The calculations are shown in detail in the appendix. Table 3 compares the proposed design procedure and the isothermal and the simple adiabatic approximations with the rigorous result with respect to this design example, and demonstrates clearly the superior accuracy of the new procedure. Figure 13 compares the rigorously computed temperature profile for this example with the estimations based on the simple adiabatic model neglecting solvent evaporation and based on the synthetic profile given in Eq. 6. Figure 13 demonstrates clearly that, due to the temperature bulge, the simple adiabatic approximation becomes useless. The ratio $(T_{L,2}-T_{L,1})/\Delta T_{max}$,

TABLE 3

COMPARISON OF RESULTS OF DIFFERENT DESIGN CALCULATIONS

Method Used	N_{OG}	Required Depth of Packing, ft
Rigorous calculation	5.56	11.90
Isothermal approximation	3.30	6.44
Simple adiabatic model	4.01	7.82
Suggested short-cut design procedure		
graphical integration	5.51	11.80
approximative anal. inte.	5.56	12.24

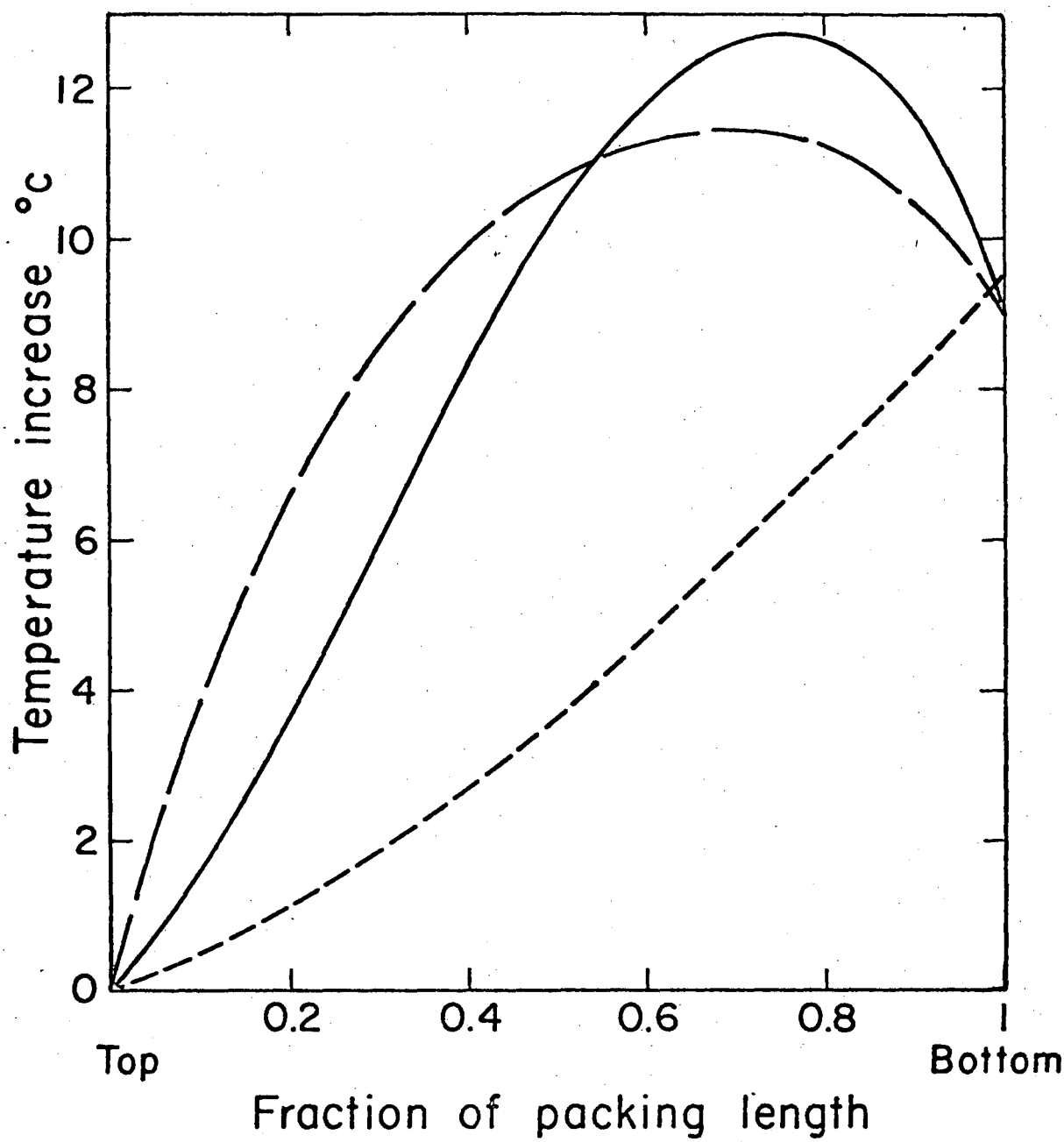

Fig. 13. Comparison of rigorous and estimated liquid temperature profile for design example XBL 764-2791

——— rigorously computed

— — — empirically constructed temperature profile Eq. 6

------- simple adiabatic model, neglecting solvent evaporation.

easily estimated from Eqs. 1 and 3 and Fig. 4, may serve as an indicator for this condition: its value is 1.3 for the present example. In cases where the ratio is large enough (say $\geq$ 4.3, compare also Fig.10), no serious temperature bulge will develop and the profile may be estimated neglecting solvent evaporation.

V. SUMMARY OF THE SHORT-CUT DESIGN PROCEDURE

Figure 14 summarizes the suggested simplified design procedure for adiabatic gas absorption in packed towers:

1) After the problem is fully specified, the temperature of the exit product is estimated using Eqs. 1 and 3 and an enthalpy balance around the tower.
2) The maximum temperature of the convex portion of the liquid temperature profile is estimated on the basis of Fig. 4 Steps 1 and 2 determine the estimated temperature profile completely.
3) The locus of the inflection point of the equilibrium curve is found by means of Fig. 10. The equation for the estimated temperature profile, Eq. 6, is then used to find the temperature as well as the slope of the equilibrium line at the inflection point. Based on this information, the effective average slopes for the two sections may be read from Figs. 8 and 9 and used in Eq. 7 to determine the necessary number of transfer units. The overall height of a transfer unit is evaluated using the effective average slopes in the usual way (Eq. 10). The total number of transfer units and the total required depth of packing are obtained by adding the respective values for the two sections together.

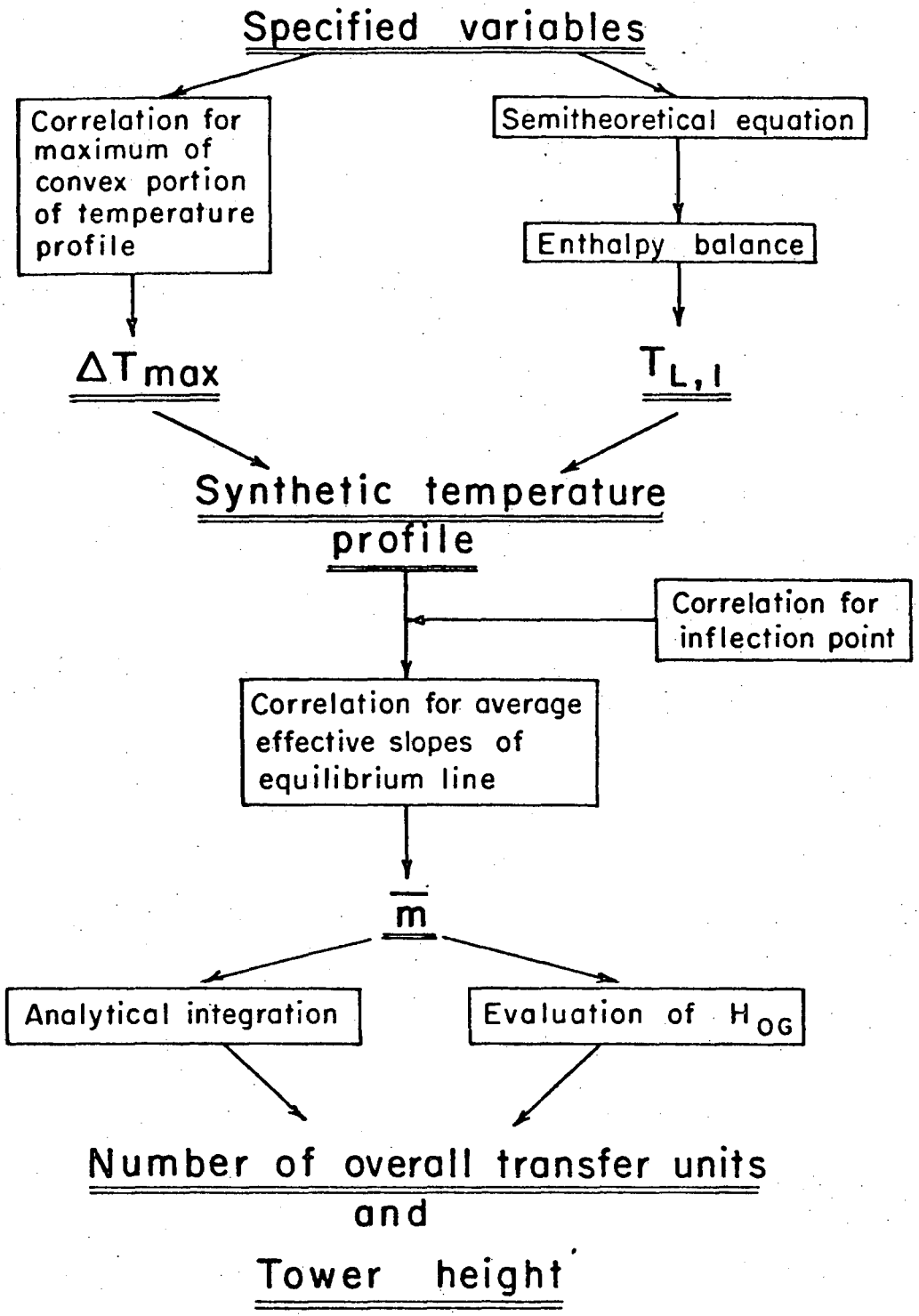

XBL753-2506

Fig. 14. Summary of suggested quick short-cut design procedure.

VI. CONCLUSIONS

The design calculations for packed columns demonstrate that heat effects normally make it impossible to design such towers approximately on the basis of any kind of simplifying assumptions. The only way to devise a quick design method, by-passing a rigorous treatment on the digital computer, is through the empirical correlation of rigorously calculated results.

Our suggested short-cut design procedure is based on such correlations and affords therefore in most cases of practical interest a much better result than that obtained with other approximate computation methods. Since the need for graphical integration is eliminated, application of the short-cut method is often even less time consuming than the conventional approximate design procedures.

The method proposed here should be particularly useful when a quick approximate estimation of the required packing height is desired and when the time consuming process of programming the problem for the rigorous treatment on the digital computer is not yet warranted.

Acknowledgement

The support received by one of the authors from "Stiftung für Stipendien auf dem Gebiete der Chemie," Basel, Switzerland is gratefully acknowledged.

APPENDIX

DESIGN EXAMPLE

The specifications of this example correspond to a problem outlined in "Mass Transfer" by Sherwood, Pigford and Wilke (4), where a conventional approximate solution is given. Consider the recovery of acetone from an acetone-air mixture by absorption in water using a scrubber packed with 1" Berl saddles. The gas is almost saturated with water at 15°C, corresponding to 0.0168 mole fraction and contains 6 mole-% acetone. The flow rate is 4000 ft^3 at 1 atm. 27,120 lb of water per hour is supplied at 15°C, corresponding to a rate 20% greater than the theoretical minimum calculated on the basis of the simple adiabatic model. Estimate the packed height required to recover 90% of the acetone and the number of overall gas phase transfer units.

Solubility The solubility of acetone in water is given by Othmer et al. (5). As shown in "Mass Transfer," (6), the data may be represented by a van Laar Equation with temperature dependent constants:

$$^{10}\log \gamma = \frac{A/T}{\left[1 + \frac{A\,X_A}{B(1-X_A)}\right]^2}$$

where

$$A = 2.3933 \cdot T - 454.43 \quad ; \quad B = 600.7 - 1.403 \cdot T \text{ (in °K)}$$

$$p_A^o = \exp\left\{-\frac{3794.06}{T} + 18.1594\right\}$$

$$m_A = X_A\,\gamma\,\frac{p_A^o}{760}$$

Mass and Heat Transfer Characteristics. If the column is specified to operate at 70% of the flooding velocity, the diameter comes out to be 4.11 ft and the gas and liquid mass velocity 1455 and 2270 lb/(hr)(ft^2). At this condition the heights of a transfer unit are (4):

$$H_{G,A} = 1.37 \text{ ft} \quad ; \quad H_L = 0.99 \text{ ft} \quad ; \quad H_{G,B} = 0.9 \text{ ft}$$

Using the Chilton-Colburn analogy, the heights of a transfer unit for heat may be estimated:

$$H_{G,Q} = 1.08 \text{ ft} \quad ; \; H_{L,Q} = 0.09 \text{ ft}$$

Thermal Data. The latent heats are estimated as (4):

$$H_{OS} = 7656 \text{ cal/(mole)} \quad ; \quad H_V = 10755 \text{ cal/(mole)}$$

For best results, the heat of solution of the solute, H_{OS}, should allow for the heat of mixing and should represent an average value at a mean concentration and temperature. The heat of vaporization, H_V, may be taken for the pure solvent at a fixed reference temperature, e.g. 0°C. (The reference temperature should, however, not be too far below the operating conditions.) The specific heats of the involved compounds are, in cal/(mole)(°C):

$$c_{pA} = 12, \quad c_{pB} = 8, \quad c_{pC} = 7 \text{ and } c_{qB} = 18.$$

Flow Rates. The gas feed rate is

$$G_{M,1} = \frac{4000}{359} \; \frac{273}{288} = 633.7 \text{ lb-moles/hr}$$

Amount of acetone recovered:

$$\Delta g_A = 0.06 \times 633.7 \times 0.9 = 34.22 \text{ lb-moles/hr}$$

The total amount of exit gas could be estimated assuming that the gas is saturated with water so that no net water evaporation occurs. Taking the saturation concentration at the top as $Y_B^* = 0.01692$, a more accurate balance shows

$$\Delta g_B = G_M \frac{Y_{B,1} - Y_{B,2}}{1 - Y_{B,2}} + \Delta g_A \frac{Y_{B,2}}{1 - Y_{B,2}} = 0.51$$

$$G_{M,2} = 633.7 - 34.22 - 0.51 = 598.97 \text{ lb-moles/hr}$$

$$\overline{G_M} = \frac{633.7 + 598.97}{2} = 616.33$$

$$L_{M,1} = L_{M,2} + G_{M,1} - G_{M,2} = 1541.43 \text{ lb-moles/hr}$$

$$\overline{L_M} = 1524.06$$

$$\left(\frac{G_M}{L_M}\right)_{av} = 0.4044$$

Concentrations and Mean Specific Heats.

$$Y_{A,1} = 0.06 \quad ; \quad Y_{A,2} = \frac{633.7 \times 0.06 \times 0.1}{598.97} = 0.006348$$

$$Y_{A,1} = \frac{34.22}{1541.43} = 0.0222$$

From these concentrations the average specific heats of the phases may be deduced:

$$c_{p,1} = 7.317 \quad ; \quad c_{p,2} = 7.048 \quad ; \quad \overline{c_p} = 7.183 \text{ cal/(mole)(°C)}$$

$$c_{q,1} = 17.867 \quad ; \quad c_{q,2} = 18.0 \quad ; \quad \overline{c_q} = 17.933 \text{ cal/(mole)(°C)}$$

STEP 1: ESTIMATION OF THE TEMPERATURE OF THE EXIT LIQUID

1. Temperature and Solvent Content of Lean Gas

From a table of water vapor pressure, dm_B/dT at 15° is found:

$$\frac{dm_B}{dT} = 0.00108, \text{ while } m_B \text{ (15°C)} = 0.01692$$

From Eq. 1

$$\frac{dT_L}{dX} = \frac{1506.7 \times 7656 - 598.97 \times 10755 \times 0.01692}{1506.7 \times 18 - 598.97 \times 7.048 - 598.97 \times 10755 \times 0.00108}$$

$$= 716.75\,°C/\text{mole fraction}$$

Both $H_{OG,A}$ and $H_{OG,Q}$ must be known at the lean end which requires knowledge of m_A at the lean end: At 15°C, the van Laar constant A is A = 235.23 °K. Since X = 0, B is of no importance and γ = 6.5512.

$$m_A = \frac{6.5512}{760} \exp\left(-\frac{3794.06}{288.16} + 18.1594\right) = 1.2703$$

$$H_{OG,A} = 1.37 + 1.2703 \frac{598.97}{1506.7} \times 0.99 = 1.87 \text{ ft}$$

$$H_{OG,Q} = 1.08 + \frac{598.97}{1506.7} \times 0.09 = 1.12 \text{ ft}$$

$$T_{G,2} = 15 + 716.75 \frac{1.12}{1.87} \frac{598.97}{1506.7} 0.006348 = 16.08°C \qquad \text{(Eq. 3)}$$

From vapor pressure tables m_B at that temperature is 0.01812. The gas will be assumed saturated with water at that temperature and at the acetone concentration $Y_{A,2}$:

$$Y_{B,2} \approx 0.0182\left(1 - \frac{0.006348}{1.27}\right) = 0.01803$$

At this point, one might improve the accuracy of the calculation by working again through the procedure suggested in section "Flow Rates" and thus adjusting the flow rates according to the new $Y_{B,2}$ but since in our case the new

value of $Y_{B,2}$ deviates only slightly from the first assumption, it is justified to omit this correction and to continue the calculation with the same average flow rates.

2. Enthalpy Balance

$$T_{L,1} \approx T_{L,2} + \left[\left(\frac{G_M}{L_M}\right)_{av} \frac{1}{\bar{c}_q} \bar{c}_p (T_{G,1} - T_{G,2}) + H_V (Y_{B,1} - Y_{B,2})\right] + \frac{H_{OS}}{\bar{c}_q} (X_{A,1} - X_{A,2})$$

$$= 15 + \left[\frac{0.4044}{17.933} 7.183(-1.08) + 10755(0.0168-0.01803)\right] + \frac{7656}{17.933} 0.0222 = 24.01°C$$

The rigorous solution on the computer yielded the following results:

$$T_{G,2} = 16.5°C \quad ; \quad Y_{B,2} = 0.0183 \quad ; \quad T_{L,1} = 24.12°C$$

STEP 2: ESTIMATION OF ΔT_{max}

The product ξ of the heating and the cooling potential is

$$\xi = 7656 \times 10755 \left(\frac{0.4044}{17.933}\right)^2 \times (0.06 - 0.006348) = 2246.5°C^2 \quad \text{(Eq. 5)}$$

The X-value to be used in the correlation shown in Figure 4 is $\sqrt{\xi} = 47.4°C$. The corresponding value on the ordinate, which may also be computed by the appropriate expression in Eq. 4 is 1.34°C.

To translate that into ΔT_{max}, the overall gas phase heights

of the transfer units should be re-evaluated at average flow rates. Since the average temperature is not know at this point, being a dependent variable, the correlation assumes that the slopes of the equilibrium lines are evaluated at the temperature of the liquid feed (15°C). The same applies for Y_B^* in the exponential expression in Eq. 4.

$H_{OG,A} = 1.37 + 1.2703 \times 0.4044 \times 0.99 = 1.88$ ft

$H_{OG,B} = 0.9 + 0.01692 \times 0.4044 \times 0.99 = 0.91$ ft (Note: $H_{L,A}=H_{L,B}$)

$H_{OG,Q} = 1.08 + 0.4044 \times 0.09 = 1.12$ ft

Substituting into Eq. 4, or into the expression given on Fig. 4:

$$\Delta T_{max} = 1.34 \times 10.039 \times 1.27^{0.995} \times 0.01692^{0.443} \times e^{0.36 \frac{0.0168}{0.01692}} \times \left(\frac{1.88}{0.91} - 0.39\right)^{0.66} \left(\frac{1.88}{1.12}\right)^{0.403} = 6.9°C$$

The rigorously computed value amounts to 6.5°C, and the maximum of the convex portion of the liquid temperature profile occurs at a normalized concentration of 0.63.

STEP 3: ESTIMATION OF EFFECTIVE AVERAGE SLOPES OF EQUILIBRIUM LINE

1. Inflection point

The location of the inflection point is now estimated using the chart Fig. 10

$$\frac{T_{L,1} - T_{L,2}}{\Delta T_{max}} = \frac{24.01 - 15}{6.9} + 1.306$$

From the diagram: $X_{N,ip} = 0.391$; $X_{ip} = 0.391 \times 0.0222 = 0.00868$

The corresponding gas phase mole fraction is computed assuming a straight operating line:

$$Y_{ip} = 0.006348 + \frac{1}{0.4044}\ 0.00868 = 0.0278$$

Applying the synthetical temperature profile, Eq. 6, the liquid temperature at the inflection point is estimated:

$$T_{L,ip} = 15 + (24.01 - 15)\ 0.391 + 6.9 \times 74.34\ (0.391^{1.074} - 0.391^{1.114})$$

$$= 25.42°C$$

At this temperature, the van Laar constants are A = 260.17 and B = 181.79°K.

Therefore,

$$\gamma = 10^{0.84992} = 7.0782 \quad ; \quad m_A = 2.173$$

$$Y^*_{ip} = 0.01886$$

Repeating these calculations at other liquid concentrations, the whole temperature profile along with the equilibrium concentrations Y^* are obtained as a function of liquid concentration. The required tower height can then be computed via a conventional graphical integration. To use the analytical approach, however, it suffices to calculate Y^* at the inflection point, at the bottom and the top of the column, and at one other arbitrary concentration, here e.g. X = 0.01, to allow computing the slope of the equilibrium line at the inflection point. The results are summarized in the table below.

X	X_N	T_L, °C	A, °K	B, °K	γ	m_A	Y^*
0	0						0
0.00868	0.391	25.42	260.17	181.79	7.0782	2.173	0.01886
0.01	0.45045	25.90	261.32	181.12	7.061	2.2142	0.02214
0.0222	1	24.01	256.80	183.77	6.484	1.875	0.04163

The slope of the equilibrium line at the inflection point is approximately

$$m_{ip} = \frac{0.02214 - 0.01886}{0.01 - 0.00868} = 2.485$$

2. Top Part of the Column

The following parameters are now computed for use in the correlation of the effective average slope:

$$m_c = \frac{0.01886}{0.00868} = 2.173$$

$$\frac{m_c}{m_2} - 1 = \frac{2.173}{1.2703} - 1 = 0.711 \quad ; \quad \frac{Y^*_{ip} - Y^*_2}{Y_{ip} - Y^*_2} = \frac{0.1886}{0.00868} = 0.6784$$

$$\frac{Y_{ip} - Y^*_2}{Y_2 - Y^*_2} = \frac{0.0278}{0.06348} = 4.3793 \quad ; \quad 4.3793^{0.1797} = 1.3039$$

Reading now from the chart shown in Fig. 8 , the value at the Y-axis turns out to be 0.717. This result may alternatively be obtained by applying Eq. 8.

$$\bar{m} = \frac{0.717}{1.3039} + 1 \quad 1.2703 = 1.969$$

$$\left(\frac{mG_M}{L_M}\right)_{eff} = 1.969 \times 0.4044 = 0.7963$$

Applying now Eq. 7: $N_{OG} = \dfrac{\ln(1-0.7963)\ 4.3793 + 0.7963}{1 - 0.7963} = 2.571$

Equation 10: $H_{OG} = 1.37 + 0.7963 \times 0.99 = 2.158$ ft

$h_T = 5.55$ ft.

3. Bottom Part of the Column

$$m_c = \frac{0.04163 - 0.01886}{0.0222 - 0.00868} = 1.6838$$

$$\left[1 - \frac{m_c}{m_{ip}}\right] = 1 - \frac{1.6838}{2.485} = 0.3224$$

$$\left[\frac{Y_1^* - Y_{ip}^*}{Y_1 - Y_{ip}^*}\right] = \frac{0.04163 - 0.01886}{0.06 - 0.01886} = 0.5535$$

$$\left[\frac{Y_1 - Y_{ip}^*}{Y_{ip} - Y_{ip}^*}\right] = \frac{0.06 - 0.01886}{0.0287 - 0.01886} = 4.60 \quad ; \quad 4.60^{0.2281} = 1.4163$$

Applying the chart shown in Fig. 9: value on Y-axis = 0.214. The result may alternatively be computed from Eq. 9.

$$\bar{m} = \left(1 - \frac{0.214}{1.416}\right) 2.485 = 2.1095$$

The concentrations in this section and as a consequence the net molar flux through the interface cannot be regarded as nearly zero. Therefore, the slope of the operating line will be computed according to Eq. 12 and substituted into Eq. 7. As a first approximation,

$$\bar{Y} = \frac{0.06 + 0.0278}{2} = 0.0439 \quad ; \quad \bar{X} = \frac{0.0222 + 0.00868}{2} = 0.0154$$

The gas enters already saturated with water, so that the overall evaporation of water in this section can be assumed small. t will therefore be taken as 1 (Eq. 3, Part I of this study)

$$\left(\frac{G_m}{L_f}\right)_{eff} = 0.4044 \frac{1-0.0154}{1-0.0439} = 0.4165 \quad ; \quad \left(\frac{mG_M}{L_M}\right)_{eff} = 0.8786$$

From Eq. 7:

$N_{OG} = 2.987$; $H_{OG} = 2.24$ ft

$h_T = 6.69$ ft

4. RESULT

$$\left(N_{OG}\right)_{\text{total}} = 2.571 + 2.987 = 5.558$$

$$\left(h_T\right)_{\text{total}} = 5.55 + 6.69 = 12.24 \text{ ft}$$

References

1. Colburn, A.P., Trans. Am. Inst. Chem. Engrs. 35, 211 (1939).

2. Bourne, J.R., U. v. Stockar, and G.C. Coggan, Ind. Eng. Chem. Proc. Des. Develop. 13, 124 (1974).

3. Wiegand, J.H., Trans. Am. Inst. Chem. Engrs. 36, 679 (1940).

4. Sherwood, T.K., R.L. Pigford, and C.R. Wilke, "Mass Transfer," pp. 616-620, McGraw-Hill Book Co., Inc., New York 1975.

5. Othmer, D.F., R. C. Collmann and R.E. White, Ind. Eng. Chem. 36, 963 (1944).

6. Wilke, C.R. and U. v. Stockar in: Sherwood, T.K., R.L. Pigford, and C.R. Wilke, "Mass Transfer," pp. 468-485 and 525-542, McGraw-Hill Book Co., Inc., N.Y. 1975.

Symbols

a	Specific interfacial surface, ft^{-1}
b	Specific holdup, lb moles/ft^3
c_p	Specific heat of a gas, cal/(mole)(°C)
c_q	Specific heat of a liquid, cal/(mole)(°C)
D_{jm}	Effective diffusivity of component j in a mixture, ft^2/hr
G_M	Molar gas flow rate, lb mole/(hr) or lb mole/(hr)(ft^2)
Δg_j	Amount of component j absorbed, lb mole/(hr) or lb mole/(hr)(ft^2)
H_G	Gas phase height of a mass or heat transfer unit, ft
H_L	Liquid phase height of a transfer unit, ft
H_{OG}	Overall gas phase height of a transfer unit, ft
H_{OS}	Integral heat of solution for solute, cal/mole
H_V	Heat of vaporization for solvent, cal/mole
h_G	Heat transfer coefficient for gas film, cal/(hr)(ft^2)(°C)
$\bar{h}_G$	Mean enthalpy of the gas, cal/lb mole
$\bar{h}_L$	Mean enthalpy of the solution, cal/lb mole
h_T	Required tower height, ft
L_M	Molar liquid flow rate, lb mole/hr or lb mole/(hr)(ft^2)
m_j	Slope of equilibrium line of component j, if without subscript, for solute
$\bar{m}$	Effective Average slope of equilibrium line for solute

N_j Flux of component j through interface, lb mole/(hr)(ft^2)

N_G Number of gas phase mass or heat transfer units

N_L Number of liquid phase transfer units

N_{OG} Number of overall gas phase mass transfer units, if without subscript, for solute

P Pressure, atm

p_j^o Vapor pressure of pure component j, atm

q Heat flux through interface, cal/(hr)(ft^2)

R_f Recovery fraction

T Temperature, °K or °C

t Net molar bulk flux per flux of solute, Eq. 3, Part I: $\frac{\Sigma N_j}{N_A}$. Absorption is counted positively.

t Time, hr

t_j Net molar bulk flux per flux of component j, Eq. 3, Part I.

ΔT_{max} Maximum of convex portion of liquid temperature profile, °C

X_j Mole fraction of component j: if j no specified, of solute

$(X_f)_j = \dfrac{(1 - t_j X_j) - (1 - t_j X_{ji})}{\ln \dfrac{1 - t_j X_j}{1 - t_j X_{ji}}}$, liquid film factor for component j; if j not specified, for solute

$X_{N,j} = \dfrac{X_j - X_{j,2}}{X_{j,1} - X_{j,2}}$, normalized mole fraction of component j; or of solute if j no specified

Y_j Mole fraction of component of component j; or of solute if j no specified

ΔY Solute concentration difference from bottom to top of column

Y_j^* Equilibrium concentration of component j, or of solute if j no specified

$(Y_f)_j$ Gas film factor of component j, Eq. 5 Part I; or of solute if j not specified

$Y_{BM} = \dfrac{(1-Y) - (1-Y_i)}{\ln \dfrac{1-Y}{1-Y_i}}$, logarithmic mean of stagnant gas concentration

$Y_f^* = \dfrac{(1-tY) - (1-tY^*)}{\dfrac{1-tY}{1-tY^*}}$, Film factor, overall driving-force basis (for solute)

z Packed height, ft

ξ Product of heating and cooling potential, Eq. 5

$\bar{\rho}$ Mean density of liquid, lb mole/ft^3

Subscripts

A Component A = solute

B Component B = solvent

C Component C = inert gas

G Gas

Q Sensible heat

eff effective

av Average

i Interphase

ip Inflection point

j Component j

L Liquid

1 Foot of absorber

2 Top of absorber

Figure Captions

Figure 1 — Liquid temperature profiles for different operating conditions and system properties

Figure 2 — Convex portions of liquid temperature profiles at different operating conditions

Figure 3 — Semitheoretical model for prediction of $T_{G,2}$

Figure 4 — Correlation of ΔT_{max}

Figure 5 — Correlation of liquid concentration at which ΔT_{max} occurs

Figure 6 — Empirically constructed, synthetic liquid temperature profile

Figure 7 — Definition of effective average slopes of equilibrium line

Figure 8 — Correlation of effective average slope $\bar{m}$ of equilibrium line. Dilute part of absorber

Figure 9 — Correlation of effective average slope $\bar{m}$ of equilibrium line. Concentrated part of absorber

Figure 10 — Correlation of inflection point

Figure 11 Comparison between rigorous solution and suggested quick short-cut design procedure

Figure 12 Comparison between rigorous solution and suggested quick short-cut design procedure analytical integration

Figure 13 Comparison of rigorous and estimated liquid temperature profile for design example

———————— rigorously computed

—— —— —— empirically constructed temperature profile Eq. 6

---------- simple adiabatic model, neglecting solvent evaporation

Figure 14 Summary of suggested rapid short-cut design procedure

TECHNICAL INFORMATION DIVISION
LAWRENCE BERKELEY LABORATORY
UNIVERSITY OF CALIFORNIA
BERKELEY, CALIFORNIA 94720